

# OPTIMIZATION OF THE COLLIMATION SYSTEM FOR THE SNS ACCUMULATOR RING

N. Catalan-Lasheras<sup>†</sup>, Y.Y. Lee, H. Ludewig, N. Simos, J. Wei  
Brookhaven National Laboratory; Upton, NY 11973, USA

## Abstract

The collimation system for the Spallation Neutron Source (SNS) accumulator ring will dissipate about 2 kW of beam power and is designed for a capture efficiency close to 95% of the halo. Preliminary studies, assuming no errors and a uniform distribution of losses, indicated that a maximum level of uncontrolled loss of 0.01% of the total beam is achievable. On the other hand, the energy lost in the primary scraper could concentrate uncontrolled losses in areas of maximum dispersion. We use Monte Carlo simulations to clarify some beam dynamic issues that could compromise the high efficiency required. The material interacting with the beam and the shape of the three structures forming the collimator system have been carefully chosen to maximize the collimation efficiency and minimize activation. Moreover, a realistic distribution of losses around the machine allows identification of potential hot points. This paper describes the latest version of the collimation system and summarizes the main results of these numerical studies.

## 1 INTRODUCTION

The future Spallation Neutron Source (SNS) is designed to deliver a proton beam with 2 MW of beam power to a liquid mercury target. The accelerator consists of a full energy (1 GeV) linear accelerator providing a  $H^-$  beam to an accumulator ring.

One of the principal requirements is to achieve hands-on maintenance and high machine availability. To allow safe and quick access to the ring, the activation of the machine components has to be kept below about 1nA, corresponding to  $10^{-4}$  of the total beam distributed uniformly around the machine [1]. On the other hand, the expected losses are of the order of  $10^{-3}$ . To achieve hands-on maintenance, we aim to control these losses, i.e., collimators are placed at strategic positions around the ring to remove particles outside the beam core and to localize losses. Ideally, these locations become the only hot spots of the machine in which remote handling is required.

## 2 CHOICE OF COLLIMATORS

The collimators designed for the ring and transfer lines of the SNS consist of a layered structure designed to capture the beam protons and any resulting radioactive isotopes within the structure of the collimator. The final structure, including external shielding, is about two meter long

and weighs more than twenty tons. A more detailed description of these collimators can be found in reference [2]. Once the collimators are installed in the machine, we can change their aperture only by replacing the vacuum pipe. While this can be done during long maintenance shutdowns if absolutely necessary, changing the aperture to adjust for changes in orbit or beam size is impossible.

Besides, the SNS accumulator ring painting scheme is designed to provide both correlated and anti-correlated painting, producing a square or round beam respectively with different emittance and beam size [3].

For the primary collimator we use a thin, movable scraper, and use the original design for the secondary collimators. Independent motors drive four collimator jaws with a thickness of about one centimeter along the beam. In this way, the position of these primary targets can be adjusted during the operation, and the shape of the collimator can be adapted to the actual beam as shown in Fig. 1. To

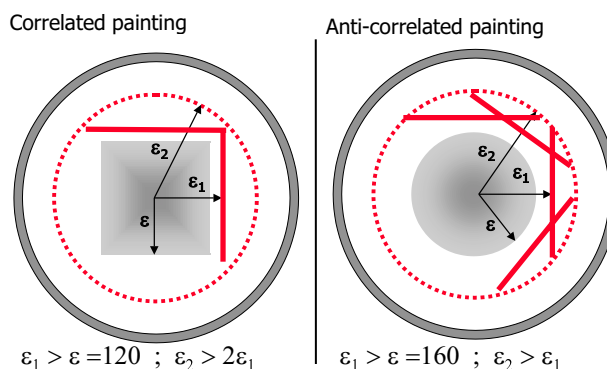


Figure 1: Schematic view of the beam, pipe and collimators in the real space  $x$ - $y$ . For both cases, correlated and anti-correlated painting are accommodated by adjusting the four scrapers of the primary collimator.

accommodate the beam we need a primary aperture  $\epsilon_1 \geq \epsilon$ , where  $\epsilon$  is the beam emittance. For the square and circular beam we have respectively  $\epsilon = 120$  and  $160\pi$  mm-mrad. To avoid having the secondary collimators receive primary impacts,  $\epsilon_2$  has to be larger than  $\epsilon_{ant}$  in the anti-correlated case and larger than  $2\epsilon_{cor}$  for correlated painting. With  $\epsilon_{1,cor} = 140$  and  $\epsilon_{1,ant} = 180$ , the minimum secondary aperture is  $\epsilon_2 = 280\pi$  mm-mrad. We chose a value of  $300\pi$  mm-mrad to allow for flexibility in the positioning of the scrapers without compromising the efficiency (see section 4). The minimum ring acceptance is  $480\pi$  mm-mrad.

At energies around 1 GeV, energy loss by ionization is non-negligible when compared with the total kinetic energy. We prefer materials with high atomic numbers which provide maximum scattering angles relative to the energy

\* Work supported by the U.S. Department of Energy

<sup>†</sup> catalan@bnl.gov

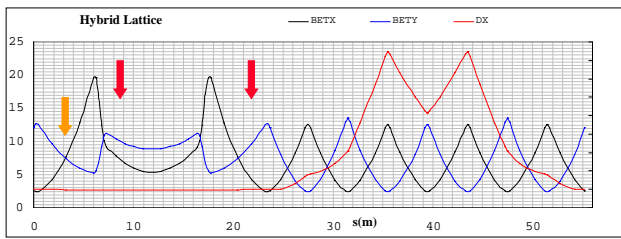


Figure 2: View of a super period in the SNS accumulator ring. The first 30 meters correspond to the straight section divided into three smaller drifts. Collimator positions are indicated by arrows.

loss. We consider thin scatterers ( $\approx 5\text{mm}$ ) of Tungsten or Platinum because they also have a high conductivity and high melting point, both of which improve the heat dissipation.

### 3 COLLIMATION SYSTEM

The accumulator ring has a hybrid lattice consisting of FODO cells in the arc and doublet cells for the straight sections. The total phase advance per straight section is about  $180^\circ$  along 30 meters. The Twiss functions along one of the four super periods are shown in Fig. 2. One of the four straight sections of the SNS ring is designated for betatron cleaning. Even if the lattice functions are common to all the machine and can not be modified in the cleaning section, the 26 meters of space available for the collimators gives a reasonable margin for optimization.

For a system whose primary and secondary collimators have normalized aperture of  $n_1 = 2.25$  and  $n_2 = 2.88$  of rms beam size, the optimum phase advances in the one dimensional case [4] are  $\mu_{opt} = \arctan n_2/n_1 \approx 52^\circ$  and its complement  $128^\circ$ . The first collimator is arbitrarily located at the middle of the first straight section. The best location for secondary collimators was found by numerical minimization of the residual halo [5]. The first secondary collimator is located in the long straight section between both doublets. The middle point of the collimator has a phase advance from the primary of  $\mu_x = 26^\circ, \mu_y = 161^\circ$  degrees. The second secondary collimator is located in the third straight section just before the matching quadrupole and the arc. Its phase advance with respect to the scraper is  $\mu_x = 43^\circ, \mu_y = 144^\circ$ . A third secondary collimator could be located at  $\mu_x = 42^\circ, \mu_y = 54^\circ$  if needed to decrease even further the uncontrolled losses. The longitudinal location for all three collimators is shown in Fig. 2.

#### 3.1 Cleaning Efficiency

With a predicted level of losses of  $10^{-3}$  due mainly to space-charge halo growth [1], the efficiency of the collimation system has to be larger than 90% to reduce the final uncontrolled loss to the  $10^{-4}$  level. We performed simulations with the K2 code [6] using a linear model of the machine and the formerly described collimation system. The inefficiency of the cleaning system ( $1 - \eta$ ) is defined as the

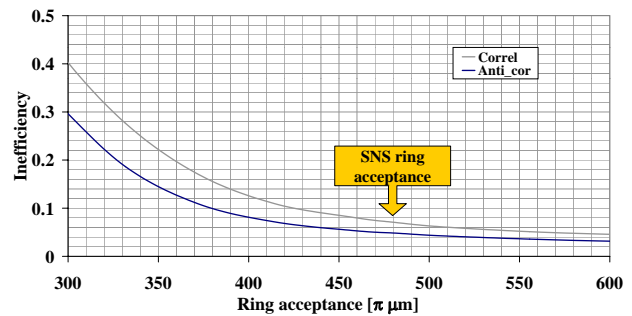


Figure 3: Integrated profile of the residual halo after traversing the collimation system. For a ring acceptance of  $480\pi\text{mm}\cdot\text{mrad}$  the inefficiency is about 5% for the correlated case and 7% for the anti-correlated.

fraction of the halo escaping the collimation system with an emittance equal to or larger than the ring acceptance. We obtain efficiencies larger than 90% for both nominal cases using two scrapers at  $\epsilon_1 = 140\pi\text{mm}\cdot\text{mrad}$  or four scrapers at  $\epsilon_1 = 180\pi\text{mm}\cdot\text{mrad}$ . The efficiency figures in both cases are 95 and 93% respectively.

### 4 FLEXIBILITY

We have designed a flexible collimation system capable of adjusting to a changing beam and reducing the uncontrolled loss to tolerable values. However, to take advantage of the flexibility of the system, we have to make sure that the efficiency is not dramatically reduced when changing the operating conditions.

#### 4.1 Tunability

As mentioned in reference [7], the SNS accumulator ring has been designed to operate at three different working points. The cleaning efficiency should not be dramatically affected by the choice of tune because most of the tuning is done in the arcs resulting in the same phase advances inside the straight section. Indeed, the residual halo profile shown in Fig. 4 for the three tune values does not present major differences. Especially in the region  $400\text{--}500\pi\text{mm}\cdot\text{mrad}$  where the ring aperture lies, the difference in efficiencies does not exceed 1% of the initial halo.

#### 4.2 Primary aperture

The location of the secondary collimators has been optimized for collimator acceptance  $\epsilon_2 = 300\pi\text{mm}\cdot\text{mrad}$  and  $\epsilon_1 = 140\text{--}180\pi\text{mm}\cdot\text{mrad}$  for correlated and anti-correlated painting respectively. Still, in the eventuality of a different beam size, we should be able to retract the primary scrapers without a significant decrease in the cleaning efficiency. Figure 5 shows the cleaning efficiency when the primary collimator is moved from its nominal position and for both collimation schemes. We see from the plot that the nominal efficiency is better for correlated painting, but it deteriorates faster with increasing  $\epsilon_1$  as the secondary

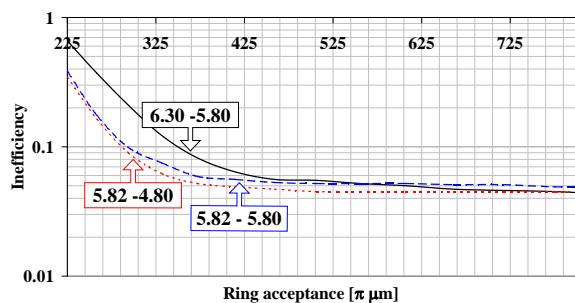


Figure 4: Residual halo profile for three different working points. The nominal tune is presented on the top curve. (Anticorrelated painting only.)

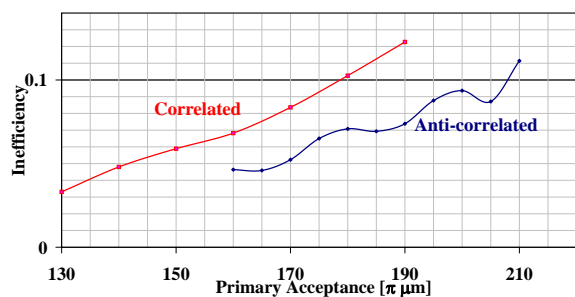


Figure 5: Cleaning efficiency as a function of the primary aperture for both cases, correlated and anti-correlated painting.

collimator becomes partially a primary. To keep the final cleaning efficiency above 90%, we can open the primary collimator up to  $205\pi\text{mm}\cdot\text{mrad}$  for a square beam and up to  $180\pi\text{mm}\cdot\text{mrad}$  for a round one.

### 4.3 Halo growth rate

When dealing with single collimators, the impact parameter has a determining role on the escape probability and thus in the final collimating efficiency. The impact parameter at the collimator depends on the drift velocity of the halo particles, which itself depends on the halo formation mechanisms and nonlinear behavior of the machine. At the present time, we do not have accurate estimates or measurements of the drift velocity for the SNS ring halo. For the simulations, the halo drift velocity in sigma per second can be adjusted by the user as a linear function of the particle emittance [8]. We studied how the result of the simulations depends on this unknown parameter. Changes of the impact parameter across three orders of magnitude had no significant effect in the final profile of the survival halo or in the cleaning efficiency.

## 5 LOSS DISTRIBUTION

We estimate the distribution of losses along the cleaning section. To probe losses, we distribute completely absorbent collimators every meter of free drift with an aperture equivalent to the vacuum pipe. We also place colli-

matoms at the entrance of each quadrupole. The results of the simulation are shown in Fig. 6. Based on these results, the structure around the scraper has been redesigned and shielding has been added before the QHB10 magnet. An estimate of the residual radiation coming from these losses is presented in reference [9]. Further work is in progress

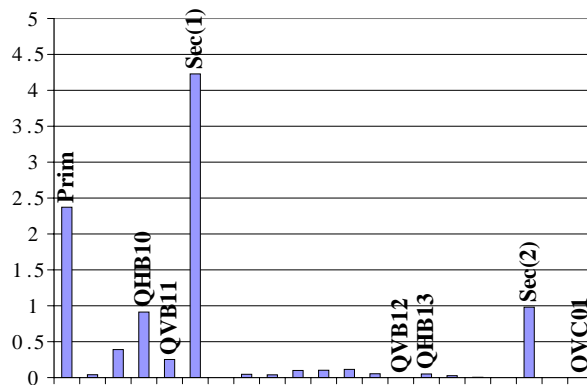


Figure 6: Loss distribution along the cleaning straight section.

to determine the losses around the ring. Special care must be taken in the the injection and extraction sections which present main aperture restrictions.

## ACKNOWLEDGMENTS

The authors would like to thank D. Kaltchev, J.B. Jeanneret, G. Rees H. Schonauer and C. Warsop for their priceless advice. Special thanks to W.T. Weng for his encouragement and support.

## REFERENCES

- [1] N. Catalan-Lasheras et al.; "Beam Loss and Collimation at SNS Ring". 7th ICFA Mini-Workshop on High Intensity High Brightness Hadron Beams; Lake Como, Wisconsin September 13-15, 1999
- [2] H. Ludewig et al.; "Collimator Systems for the SNS Ring". PAC 1999, New York, 1999
- [3] J. Beebe-Wang et al.; "Beam Properties in SNS Accumulator Ring due to Transverse Phase Space Painting", this proceedings.
- [4] J.B. Jeanneret, "Optics of a two-stage collimation system" Phys. Rev. ST Accel. Beams 1, 081001 (1998)
- [5] D. Kaltchev; "Numerical optimization of collimator jaw orientation and locations in the LHC". PAC 1997, Vancouver
- [6] T. Trenkler, J.B. Jeanneret, SL Note 94-105 (AP)
- [7] J. Wei et al., Phys. Rev. ST Accel. Beams
- [8] L. Burnod et al. LHC Note 117, 1990
- [9] H. Ludewig et al.; "Preliminary Estimates of Dose and Residual Activation of Selected Components in Ring Collimation Straight of the SNS", this proceedings